Front. Optoelectron. 2017, 10(4): 378–387
DOI 10.1007/s12200-017-0706-8

RESEARCH ARTICLE

Extracting the time delay signature of coupled optical chaotic systems by mutual statistical analysis

Xinhua ZHU, Mengfan CHENG (✉), Lei DENG, Xingxing JIANG, Deming LIU

Next Generation Internet Access National Engineering Laboratory (NGIA), School of Optical and Electronic Information, Huazhong University of Science and Technology, Wuhan 430074, China

Abstract The time delay (TD) signature is a critical parameter in optical chaos-based applications. The feasibility of extracting the TD has been a crucial issue that significantly influences the performance of these applications. In this paper, statistical analyses have been conducted to extract the TD signatures from different types of coupled optical chaos systems. More specifically, a mutually coupled semiconductor laser chaotic system, an intensity-coupled electro-optic chaotic system, and a phase-coupled electro-optic chaotic system are studied in detail. These systems are proposed to resist the attack strategies against the TD signature. They are proved to be effective under statistical analyzes, such as the self-correlation function (SF) and mutual information (MI). However, only a single output has been considered for the attack process in the existing research. We demonstrated that the TD signature can still be extracted by analyzing the mutual statistical relationship between the different output signals which are generated simultaneously by the coupled system. Furthermore, we find that the extraction strategy is effective for a wide parameter range in these schemes.

Keywords optical chaotic system, chaos, electro-optic nonlinear system, time delay (TD) concealment

1 Introduction

The chaotic dynamics of optical systems have attracted considerable attention because of their advantages, such as broad bandwidth, large transmission capability, and high level of privacy [1–7]. The commonly used method to obtain an optical chaos signal is to introduce additional degrees of freedom to semiconductor lasers (SL). Several schemes have been developed based on the delayed feedback strategy [8–12]. Those schemes either utilize the intrinsic nonlinearity of the SL or involve externally introduced nonlinear mechanisms. These optical chaotic systems have impressive applications in fields like secure communications [13–15], fast physical random bit generation [16,17], and chaotic radars [18,19]. Methods using external cavities or feedback loops can produce higher dimensional chaotic signals, but they introduce periodic components at the same time so that the chaotic output may contain a time delay (TD) signature. From a secure communication point of view, using the information of the TD signature, the chaotic carrier could be reconstructed by the attacker and the dimension of the key space could be reduced [20,21]. This will result in a significant degradation of the security level. For random bit generation, the existence of the TD signature will also limit the choices of sampling periods and affect the statistical performance [22]. Although the TD is a sensitive factor in these applications, it can be identified using statistical methods such as the self-correlation function (SF) [23], mutual information (MI) [24], the singular values fraction measure, the filling factor analysis, and neural network [25,26].

The TD signature is minimized by controlling the feedback strength and frequency detuning. Therefore various modified feedback approaches for TD signature suppression have been proposed, e.g., fiber Bragg grating (FBG) feedback [27] and polarization rotated feedback [28,29] systems. The TD signature can be suppressed due to the influence between the SL and external feedback. However, the TD signature cannot be eliminated completely since the feedback device is passive [30]. Therefore, researchers have designed cascade laser configurations. The master-slave-cascade configuration schemes [31,32] can suppress the TD signature through the interaction between the chaotic oscillation in the master and slave SLs. In particular, an external cavity laser with an

Received February 20, 2017; accepted July 13, 2017

E-mail: chengmf@mail.hust.edu.cn

optical chaos injection can generate a broadband signal without a TD signature in both the intensity and phase time series [33]. These kinds of systems use active devices, such as slave lasers, to replace the passive mirrors or FBGs, and are a relatively effective way to eliminate the TD signatures.

The post-processing method is another way to deal with the TD signature. The chaos output is post-processed by different mechanisms. For example, the optical chaos is injected into a delayed interferometer [34] or a fiber ring resonator [35]. The physical process arises in the interferometer rather than in the laser cavity. The optical heterodyne [36] and the electrical heterodyne schemes [4] use the chaotic signal to heterodyne with another chaotic signal or a single frequency local oscillator. The superposition of the chaotic spectra not only broadens the bandwidth of the original chaotic signal but also reduces the TD signature in the heterodyned chaotic signals.

More recently, the mutually coupled chaotic systems have become a popular research topic due to their unique advantages [30,37–40]. This type of system can generate two or more chaotic signals simultaneously, while the TD signature is completely suppressed. Moreover, the synchronization scheme is relatively easier to design by utilizing such coupled mechanisms. Various secure communication systems have been designed and demonstrated on the basis of this mechanism [39,40]. However, the TD signature analyses in the literature are focused only on the time series of a single output, and the mutual statistical features between different outputs is ignored. In this paper, we conduct an investigation into coupled chaotic systems, namely; the mutually coupled semiconductor [30,37], the intensity-coupled electro-optic [38], and the phase-coupled electro-optic chaotic systems [39]. Using theoretical models and experiments, two or more sets of chaotic signals transmitted in separate channels were captured or reconstructed, and the TD signature was extracted by mutual statistical analysis.

2 System models and results

2.1 Mutually coupled semiconductor laser chaotic system

This type of scheme was first proposed in Ref. [30], and the configuration of the system is illustrated in Fig. 1. Two similar SLs are subjected to one another. The polarization controller (PC) is used to match the polarization states of the two lasers, and the variable attenuator (VA) is used to control the coupling strength which is defined as the optical power ratio of the external injection light and the solitary SL output light. The photo-detectors (PD) are used to capture the TD signature, and eliminate it from the chaotic signal. In our scheme, the two outputs from the mutually coupled lasers are captured simultaneously to conduct an offline mutual statistical analysis.

The mathematical model of this mutually coupled semiconductor laser chaotic system can be expressed by the rate equations (Eqs. (1)–(3)):

$$\dot{E}_1 = \frac{1}{2}(1+\mathrm{i}\beta_1)\left[\frac{g_1\left(N_1(t)-N_0\right)}{1+\varepsilon E_1(t)^2}-\frac{1}{\tau_{p1}}\right]E_1(t) + \eta E_2\left(t-\frac{\tau}{2}\right)\mathrm{e}^{-\mathrm{i}2\pi\left(\frac{f_2\tau}{2}+\Delta f t\right)} + F_1(t), \tag{1}$$

$$\dot{E}_2 = \frac{1}{2}(1+\mathrm{i}\beta_1)\left[\frac{g_2\left(N_2(t)-N_0\right)}{1+\varepsilon E_2(t)^2}-\frac{1}{\tau_{p2}}\right]E_2(t) + \eta E_1\left(t-\frac{\tau}{2}\right)\mathrm{e}^{-\mathrm{i}2\pi\left(\frac{f_1\tau}{2}-\Delta f t\right)} + F_2(t), \tag{2}$$

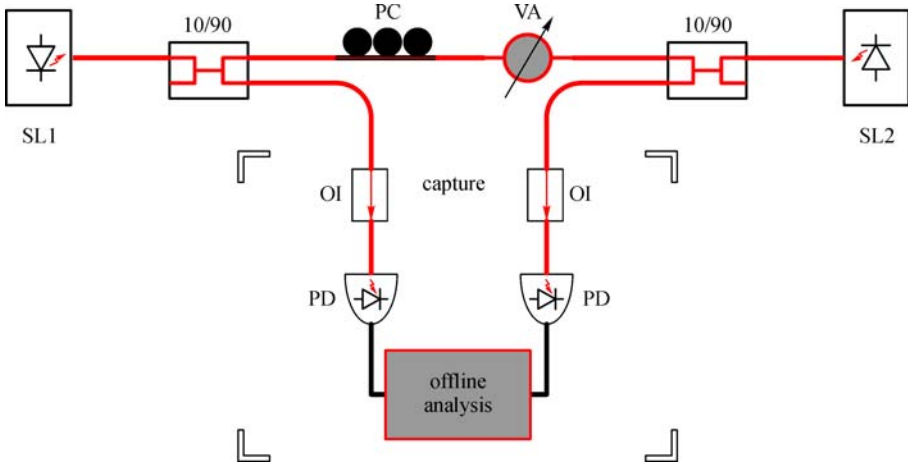

Fig. 1 Configuration of the capture system

$$\dot{N_{1,2}}(t) = J - N_{1,2}(t)/\tau_N - \frac{g_1\left(N_{1,2}(t)-N_0\right)}{1+\varepsilon E_{1,2}(t)^2}|E_{1,2}(t)|^2. \quad (3)$$

Here E is the slowly varying complex electric field; N is the average carrier number in the active region of the SL; the subscripts 1 and 2 refer to SL1 and SL2; β is the linewidth-enhancement factor; τ is the coupling round-trip time, which is the time that the output from SL1 is injected into SL2 and then feedbacks to SL1; $\tau/2$ is the delay time of the output of SL2 as it is injected into SL1 or otherwise; η is the coupling strength; the frequency detuning Δf is defined as $\Delta f = f_1 - f_2$, where f_1 and f_2 are the optical frequencies of the free running SL1 and SL2, respectively; N_0 is the transparency carrier number; and, $F_1(t)$ and $F_2(t)$ are the spontaneous-emission noises of SL1 and SL2, respectively. Considering that the parameters in Eqs. (1)–(3) are either large or small, we can express these rate equations in dimensionless form. In our simulation, the parameters were chosen in the same as those in Ref. [37].

The analyzes in Ref. [37] contain the influence of the coupled strength and frequency detuning on the TD signature. By controlling the coupled strength η, the system can effectively suppress the TD signature, which is gradually attenuated with an increase in η. When η reaches a certain value, the TD signatures are suppressed closely with the background. By continuously increasing η, the TD signature will re-appear. These results were produced using the analysis of single outputs.

In the mutually delay-coupled semiconductor laser (MDC-SL) system, two sets of TD signature suppressed chaotic signals are generated simultaneously. It was proposed that the cross correlation function (CCF) could be used to analyzes the rings of the delay-coupled elements [41]. In our work, the Eqs. (1)–(3) are numerically simulated using MATLAB R2012A and the fourth order Runge-Kutta algorithm with 10^6 data points (from 10^6 to 2×10^6) of the captured time series. The mutual statistical analysis CCF and delayed mutual information (DMI) between different outputs have been conducted based on E_1 and E_2 (the captured optical intensities of SL1 and SL2, respectively) for η = 7.5 ns^{-1} and Δf = 0 GHz. Other parameters used were a linewidth-enhancement factor of β = 4, coupling round-trip time τ = 8 ns, $g = 2 \times 10^4$ s^{-1}, $N_0 = 1.25 \times 10^8$, and $\varepsilon = 1.5 \times 10^{-7}$. The remaining parameters were chosen as the same as those in Ref. [37].

The formulas for the CCF and DMI are given by Eqs. (4) and (5), respectively, where $V_1(i)$ and $V_2(i)$ represent the two time series, F_s is the sampling rate, $\langle\cdot\rangle$ is the time average, and $p(v_1(i))$ and $p(v_1(i), v_2(i-sF_s))$ are the mean probability distributions of the marginal and joint fault probability distributions respectively:

$$C(s,v_1,v_2) = \frac{\langle [v_1(i)-\langle v_1(i)\rangle][v_2(i-sF_s)-\langle v_2(i)\rangle]\rangle}{\{[v_1(i)-\langle v_1(i)\rangle]^2[v_2(i-sF_s)-\langle v_2(i)\rangle]^2\}^{\frac{1}{2}}}, \quad (4)$$

$$I(s,v_1,v_2) = \sum_{v_1}\sum_{v_2} p(v_1(i),v_2(i-sF_s)) * \log\frac{p(v_1(i),v_2(i-sF_s))}{p(v_1(i))p(v_2(i-sF_s))}. \quad (5)$$

The SF of E_1, the MI of E_1, and the CCF and DMI between E_1 and E_2 are illustrated in Fig. 2. As shown in Figs. 2(a) and 2(b), the TD signature was successfully eliminated in E_1 for the SF and MI analysis. However, there was an obvious peak at t = 4 ns = $\tau/2$ for CCF, as shown in Fig. 2(c). A similar TD signature was also be observed for DMI, which is shown in Fig. 2(d).

We also investigated the change of the TD signature in the parameter space where the coupling strength and frequency detuning vary. From Fig. 3, it was seen that peak values of CCF and DMI are "U" shaped. Even when a parameter was located under the "U" region, which implied that the peak value had hit a relatively low, the peak remained obvious. The specific analysis of the TD extraction for the large Δf case is illustrated in Fig. 3. The CCF and DMI curves for η = 0.04 and Δf = 12 GHz; and, η = 0.08 and Δf = 0 GHz, were analyzed. It was seen that the TD signature can still be extracted for large Δf. This can be seen in Fig. 2 for a peak value larger than 0.2. For the CCF and DMI analyses of the two transmitted time series, the TD information was still revealed for the mutually coupled semiconductor. We performed an additional analysis regarding the internal parameters of the LD. The typical value of the linewidth enhancement factor was 1 to 10. We set different values for the linewidth enhancement factor of the LDs of the coupled optical chaotic systems. Similar results were obtained. The linewidth enhancement factor is an important parameter which affects the performance of the LD, and has attracted the most attention. The other internal parameters had a relatively smaller impact. The mismatches of the internal parameters in the considered range did not affect the performance of the TD extraction under the mutual analysis of the multiple outputs.

The system developed is based on the external cavity feedback semiconductor laser (ECF-SL) system [30] and uses a semiconductor laser to replace the external cavity mirror. In other words, the SL2 is not a passive linear mirror but an active nonlinear device. By adjusting the parameters of SL2, the nonlinearity of the regenerated signal from SL2 is largely increased, compared with that of the incident signal from SL1. Thus, the TD signature cannot be obtained using the SF analysis from a single output. However, from the rate equation, the output signals of SL1 and SL2 are strongly related. The statistic feature

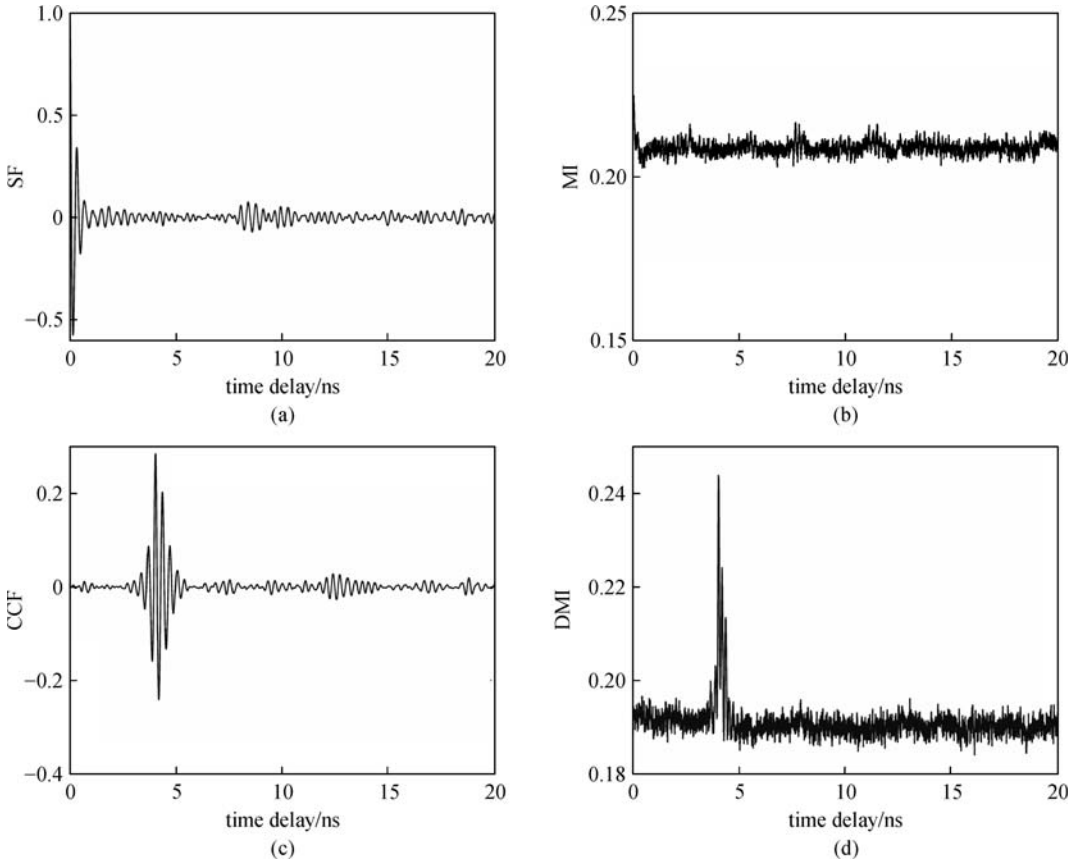

Fig. 2 (a) SF curve of E_1; (b) MI curve of E_1; (c) CCF between E_1 and E_2; (d) DMI between E_1 and E_2. Parameters are chosen at $\eta = 7.5$ ns^{-1} and $\Delta f = 0$ GHz

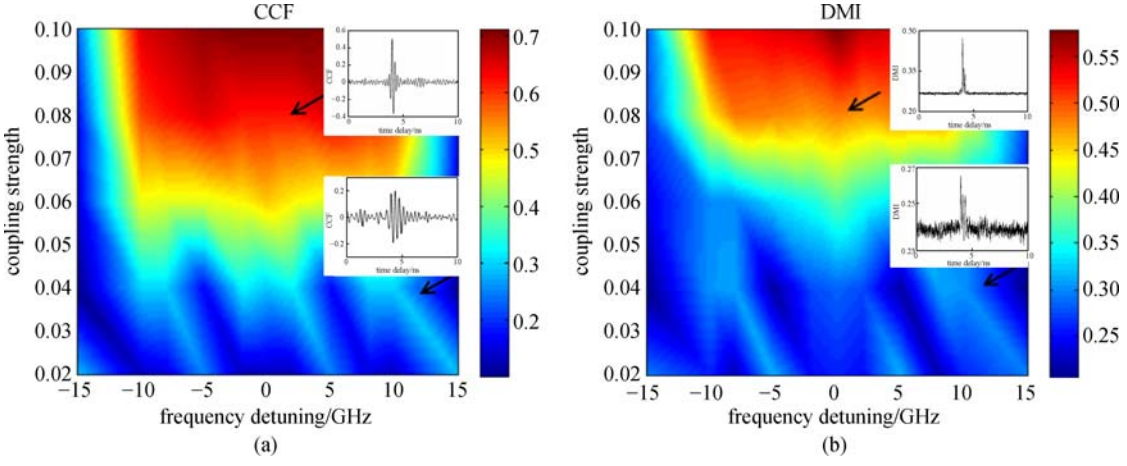

Fig. 3 Maps of TD signature in parameter space of η, Δf under CCF and DMI analyses. (a) CCF; (b) DMI. The insets show the CCF and DMI curves at $\eta = 0.04$, $\Delta f = 12$ GHz and $\eta = 0.08$, $\Delta f = 0$ GHz, respectively

between the two chaotic outputs exist, and as a result, the TD signature can be observed from the two captured time series.

2.2 Intensity-coupled electro-optic chaotic system

Unlike the chaotic lasers which are based on the intrinsic nonlinearity of the semiconductor laser, another type of extensively studied optical chaos source is based on the external nonlinear components, such as a Mach-Zehnder modulator (MZM). Coupled chaotic systems based on this strategy have also been proposed and investigated in Refs. [38,40]. The system configuration built using the intensity-coupled electro-optic chaotic system is illustrated in Fig. 4.

The system consists of three continuous-wave lasers. Each laser output is first modulated by a MZM, then detected and amplified by a PD and a radio-frequency (RF) driver, respectively, before being fed-back into the RF interface of the MZM. These devices form an electro-optic chaotic chain. Electrical splitters (ES) and electrical couplers (EC) were adopted to export the power of each chain to the other two, then the three chaotic chains were coupled to each other. The results in Ref. [38] show that the system can produce TD signature eliminated chaotic outputs.

The dynamical equation of the system is described as Eq. (2) in Ref. [38], where $x_i(i) = \pi V(t)/2V_\pi$ represents the dimensionless variable, and β is the bifurcate parameter. The other parameters are: $\Phi = \pi/4$, $\tau = 25$ ps and $\theta = 5$ μs. The TD introduced by the delay lines; DL1, DL2, and DL3, in the three chains were set to $T_1 = 30$ ns, $T_2 = 25$ ns, and $T_3 = 20$ ns, respectively. In a practical system, TD is inevitable because of the latency of the components like the MZ and PD. This latency is small enough that it can be neglected in our simplified model when compared with the TD introduced by the optical fiber.

Reference [38] indicates that the peak remains distinguishable in SF and MI, and β = 2–3.8 and 2–3.4, respectively. When β reaches 6, the peaks for the relevant TD were buried in the background, which are safe enough under attack. In our scheme, the output signals from two separate chains, for example (x_1, x_2), and (x_1, x_3) were captured. We used the mutual statistical strategies CCF and DMI to analyze the statistical properties between the two chaotic series. We first investigated the properties of the chaotic signals for β = 4, and the results are shown in Fig. 5. The peaks are buried in the background for SF and MI. However, there are obvious peaks for the CCF and DMI results of (x_1, x_2). The peak at $t = T_1 = 30$ ns is obvious when β = 4. There is also a peak at $T' = 5$ ns, which is equal to the value of T_1–T_2.

According to the results in Fig. 6, the value of β still has a great influence on the peak values of the CCF and DMI curves. When $\beta = 6$, the peak was still apparent, though the absolute value decreased. When β increased to 9, the values of the peaks of CCF(x_1, x_2) and DMI(x_1, x_2) continued to decrease. The reason for this could be that the increase in β enhanced the nonlinearity of the chaotic outputs, and therefore, suppressing the TD signature in each chain. However, the correlation between different chains was still relatively strong. As a result, the peak was obvious enough to identify the TD at $t = T_1$ even for large β. Similar results were obtained by analyzing (x_2, x_1), (x_1, x_3), (x_3, x_1) etc., and, T_2, and T_3 were also identified. Since the value of β is limited by the amplifier's gain, laser power, and half wave voltage of the MZM, it is difficult to obtain such a high value of β in real world applications. This implies that the system is not safe enough for the concealment of the TD using a mutual statistical analysis. Unfortunately, when this type of chaotic system is used in secure communications, at least two sets of chaotic carriers are needed for constructing the synchronization scheme. Therefore, multiple TDs could be partially identified and the key space of the system will be significantly reduced.

2.3 Phase-coupled electro-optic chaotic system

A phase modulated delay dynamical system is another optical chaotic source with external nonlinear devices. Phase-coupled electro-optic chaotic systems have also been proposed to resist a TD signature attack. The phase-coupled scheme was first proposed in Ref. [39]. As shown in Fig. 7, the system is composed of two connected electro-optic delayed feedback chains, which is different from the aforementioned 3-dimensional intensity-coupled strategy. However, a pseudo-random bit sequence (PRBS) is coupled to the system by the phase modulator (PM) which is an additional dimension. Since the PRBS can be generated synchronously in the transmitter and the receiver side, only a one dimensional chaotic signal is transmitted in the optical link as the information carrier. This means the eavesdropper cannot obtain two sets of chaotic signals simultaneously, which makes the mutual statistical analysis hard to perform. To overcome this problem, we designed a bypass to reconstruct an additional output, as shown in Fig. 7. The bypass configuration contained an open loop which was similar to the original chain. The PD3 was used to capture the reconstructed output.

The dynamics of the phase-coupled system can be

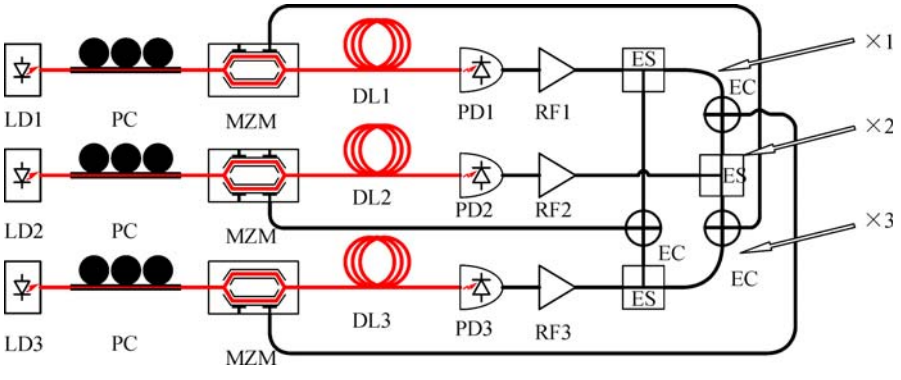

Fig. 4 System configuration built on the intensity-coupled electro-optic chaotic system

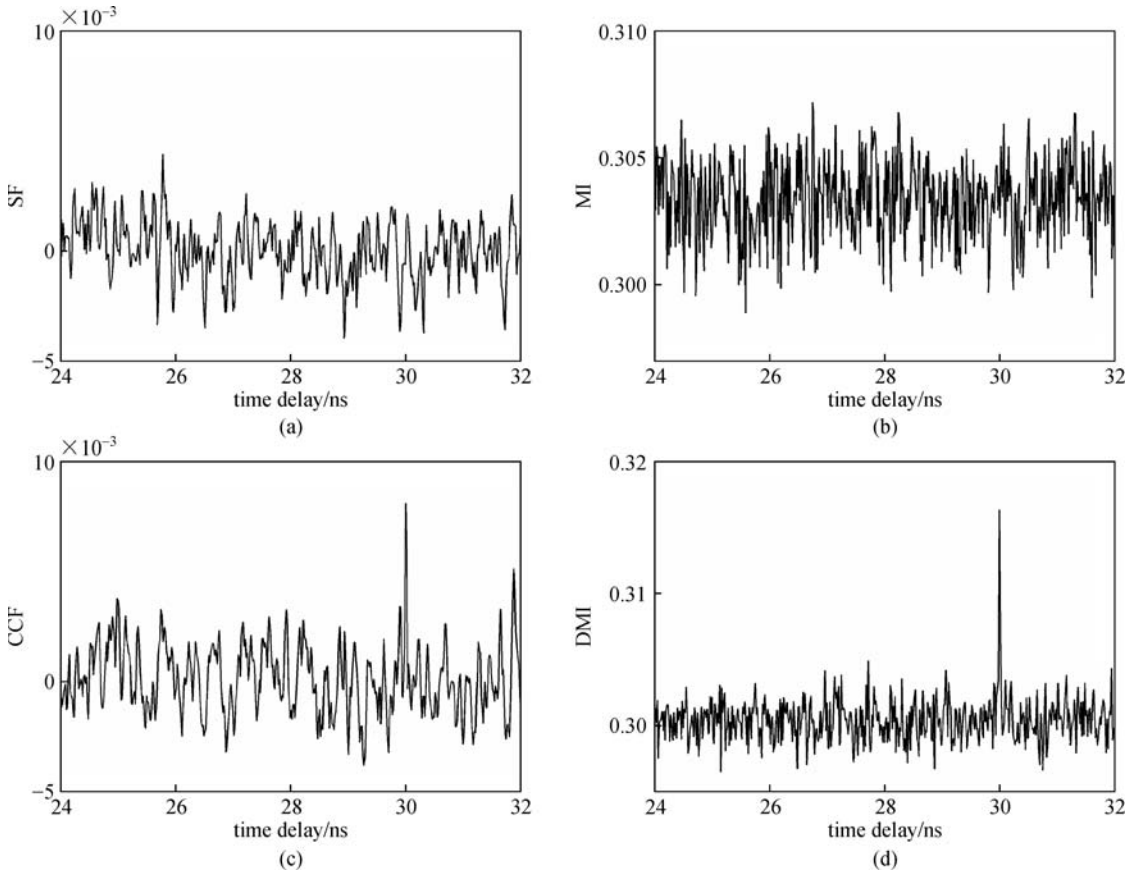

Fig. 5 SF(x_1), MI(x_1), CCF(x_1, x_2) and DMI(x_1, x_2) curves when $\beta = 4$. (a) SF curve; (b) MI curve; (c) CCF curve; (d) DMI curve

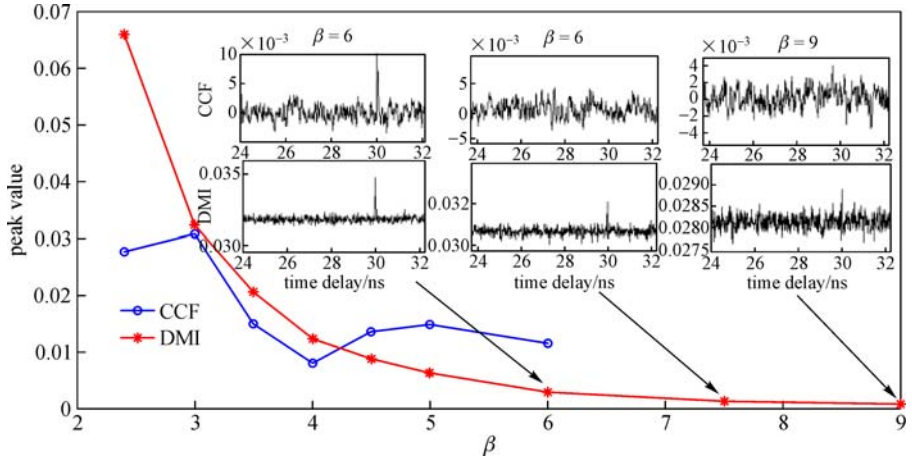

Fig. 6 Peak values of the CCF and DMI curves while β ranges from 2 to 9. The insets show the CCF and DMI curves while $\beta = 6, 7.5, 9$

modeled using Eqs. (6)–(7):

$$x_1 + \tau_1 \frac{\mathrm{d}x_1}{\mathrm{d}t} + \frac{1}{\theta_1} u_1 = \beta_1 \cos^2\left(\Delta(y_2 + R)_{T_1} + \phi_1\right), \quad (6)$$

$$y_2 + \tau_2 \frac{\mathrm{d}y_2}{\mathrm{d}t} + \frac{1}{\theta_2} u_2 = \beta_2 \cos^2\left(\Delta(x_1 + m)_{T_2} + \phi_2\right). \quad (7)$$

In the above equations $\Delta(F)_{t_0} = F(t - t_0) - F(t - t_0 - \delta t_0)$. The phase output in each chain is a mixture of the PRBS (or the R and m) and the nonlinear delayed series of the other chain. The following parameters were set at; T_1 = 15 ns, T_2 = 17 ns, δT_1 = 510 ps, and δT_2 = 400 ps. As described in Ref. [39], the TD signatures can be identified by calculating the SF and MI at $x_1(t)$. For the injection of a 3 Gb/s PRBS, the peaks were hidden in the background.

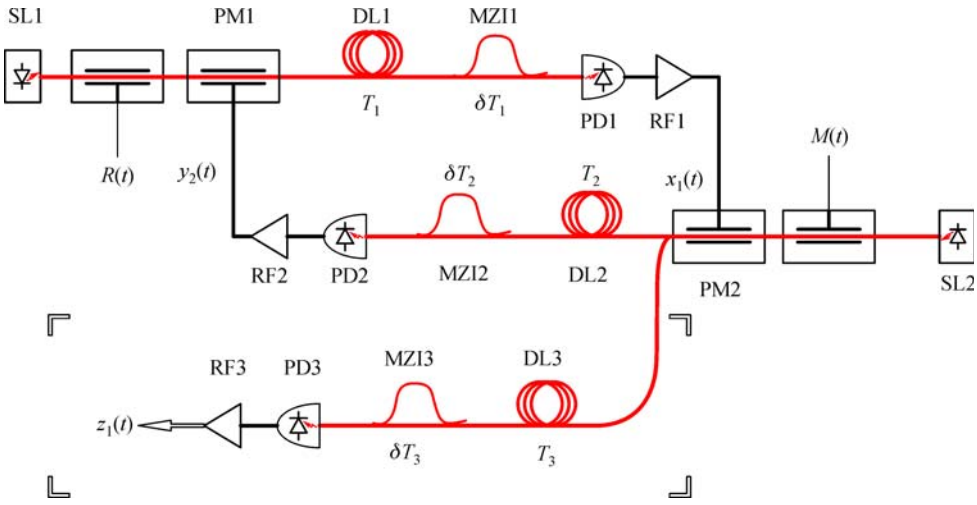

Fig. 7 System configuration built on the phase-coupled electro-optic chaotic system

We intended to extract the TD signatures by analyzing the mutual correlation between $x_1(t)$ and $y_2(t)$, however, these two signals could not be captured simultaneously, since only one carrier was needed to establish the synchronization based communication strategy. The mathematical model of the constructed bypass can be expressed by Eq. (8):

$$z_1 + \tau_3 \frac{\mathrm{d}z_1}{\mathrm{d}t} + \frac{1}{\theta_3} u_3 = \beta \cos^2\left(\Delta(x_1)_{T_3} + \phi_3\right), \qquad (8)$$

where T_3 is the value of the introduced delay line; δT_3 represents the delay introduced by MZI; and, τ_3, θ_3, ϕ_3 were chosen using typical values. The values of T_3, δT_3 were arbitrarily chosen by the attacker and we set $T_3 = 21$ ns, $\delta T_3 = 600$ ps.

In the simulation, the amplitude of PRBS was chosen as $\pi/2$ to maximize the cover efficiency, which is the same treatment as described in Ref. [39]. The following parameters were set: $\beta_1 = \beta_2 = 5$, $\beta = 4$, $\tau_1 = 20$ ps, $\tau_2 = 12.2$ ps, and $\theta_1 = \theta_2 = 1.6$ μs; and 10^7 data points (from 10^7 to 2×10^7) were used. The CCF and DMI were used to analyze the statistical properties between $x_1(t)$ and $z_1(t)$.

As shown in Figs. 8(a) and 8(b), the SF and MI curves showed no distinguishable peaks for a relevant time, but the CCF and DMI curves both had peaks at $t = T_1' = 11$ ns and $t = T_2' = 11.4$ ns, while the bit rate of PRBS was 3 Gb/s. Therefore $T_1' + T_3 = 32$ ns $= T_1 + T_2$ and $T_2' + T_3 = 32.4$ ns $= T_1 + T_2 + \delta T_1$. The influence of the bit rate of PRBS and β for the extraction was also analyzed and the results are shown in Fig. 9. It was seen that the absolute value of the peaks in the CCF and DMI curves decreased while the bit rate of PRBS increased. However, the peaks were still distinguishable when the bit rate reached the relatively large value 5 Gb/s. Even when the bit rate of PRBS increased to 10 Gbps, the TD signature was eliminated for the CCF case, but the peaks in the DMI curve were still distinguishable. In a practical system, the bit rate of the PRBS will not be as limited by the devices. Therefore, it can be concluded that the phase-coupled electro-optical chaotic system is not secure enough for the CCF and DMI analyses. We also changed the parameters of the reconstructed part, for example, β ranged from 2 to 6 and $\varepsilon = \tau/\theta$ was set to 6.25×10^{-4} and 2.5×10^{-5}, producing similar results. The CCF and DMI curves also reveal the peaks for a relevant TD. These results indicated that we can obtain parts of the TD values of the phase-coupled electro-optical chaotic system. However, the complete solution is unattainable, the range of the TDs can be narrowed down and the search space can be reduced accordingly. This vulnerability may cause degradation in the security performance.

3 Conclusions

In summary, we have conducted a mutual statistical analysis on a series of typical chaotic sources which were designed by adopting a system coupling strategy. These systems were proven to be effective in resisting the statistical attack. For these schemes, the TD signature in each single output was concealed under the SF and MI analyses. However, we have demonstrated that the TD signature can still be extracted by analyzing the mutual statistical relationship between multiple different outputs. The simulation results indicated that these systems are not safe for a wide parameter range if two or more output signals are obtained by the eavesdropper. Unfortunately, in some schemes such as the intensity-coupled electro-optic chaotic system, more than one set of chaotic signals are transmitted simultaneously in the optical link to maintain the synchronization between the transmitter and the receiver. In the phase-coupled system, the attacker can build a bypass configuration to construct a relative carrier,

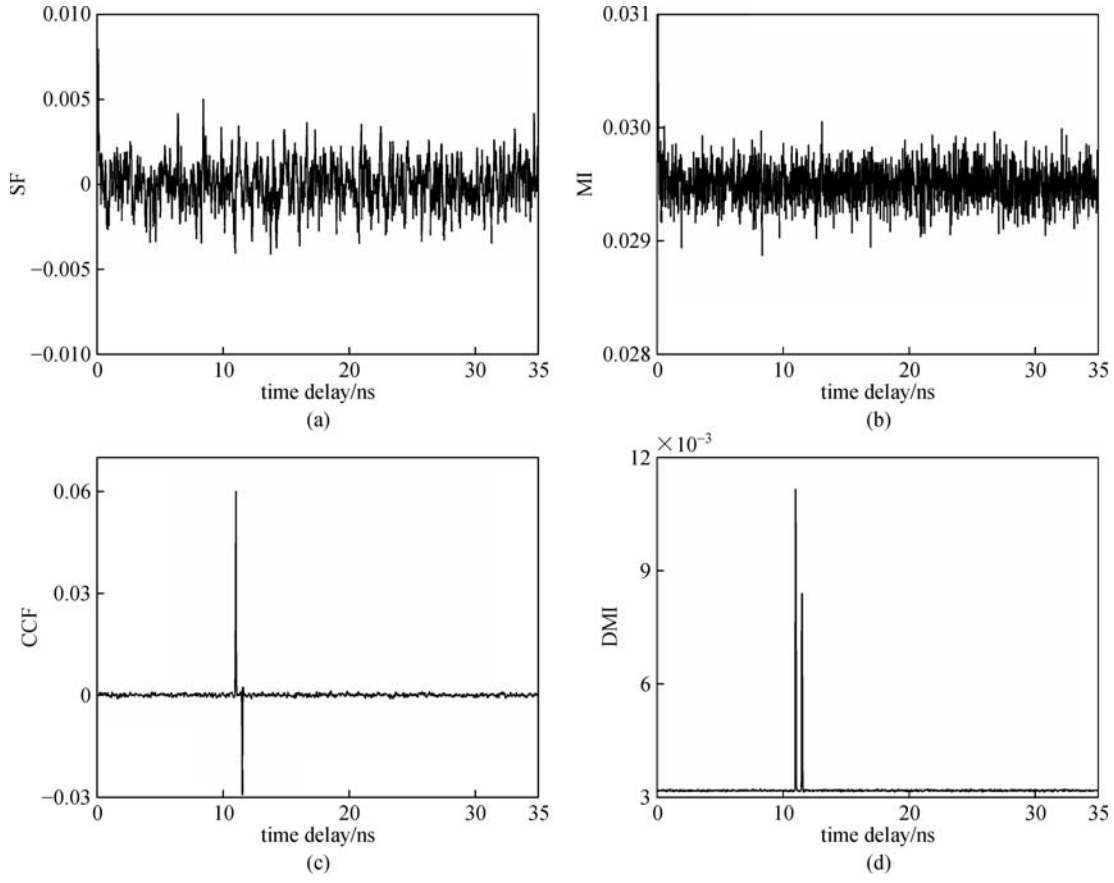

Fig. 8 SF, MI curves of $x_1(t)$ and CCF, DMI curves of $x_1(t)$, $z_1(t)$, while the bit rate of PRBS is 3 Gb/s and the amplitude is $\pi/2$. (a) SF curve; (b) MI curve; (c) CCF curve; (d) DMI curve

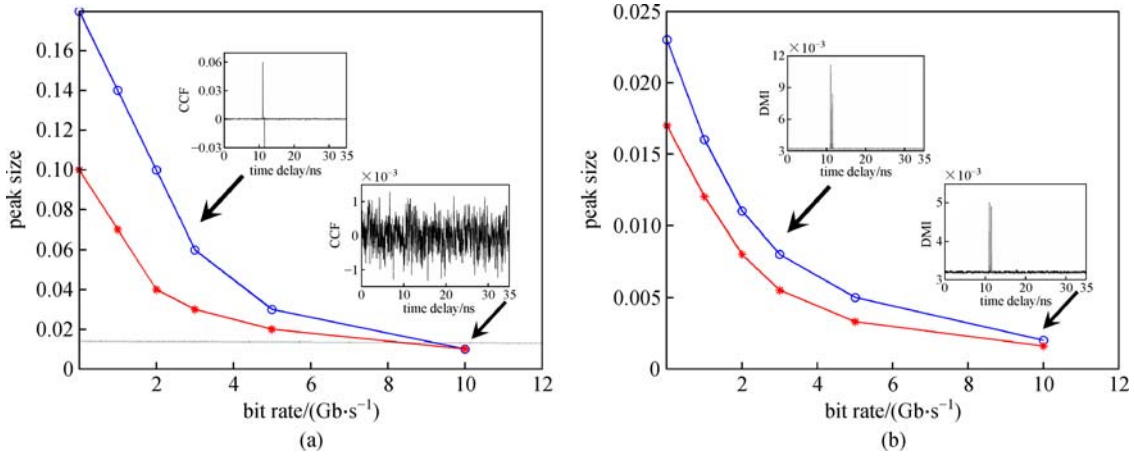

Fig. 9 Absolute value of the peaks in CCF and DMI at T_1' and T_2' while the bit rate of PRBS increases. (a) CCF; (b) DMI. The insets show the CCF and DMI curves while the bit rate of PRBS is 3 and 10 Gb/s, respectively

and the TD signature can be partially identified by using similar methods. Even though system coupling is a widely used strategy in optical chaos communication systems, the results in this paper challenge the security of this kind of system. We suggest that a mutual statistical analysis should be considered in designing the chaotic source in future works.

Acknowledgements This work was supported by the National Natural Science Foundation of China (NSFC) (Grant No. 61505061) and the National

High Technology Research and Development Program ("863" Program) of China (Nos. 2015AA016904, and 2015AA015502).

References

1. Nguimdo R M, Colet P. Electro-optic phase chaos systems with an internal variable and a digital key. Optics Express, 2012, 20(23): 25333–25344
2. Hong Y, Paul J, Spencer P S, Shore K A. Ghz bandwidth message transmission using chaotic vertical-cavity surface-emitting lasers. Journal of Lightwave Technology, 2009, 27(22): 5099–5105
3. Argyris A, Syvridis D, Larger L, Annovazzi-Lodi V, Colet P, Fischer I, García-Ojalvo J, Mirasso C R, Pesquera L, Shore K A. Chaos-based communications at high bit rates using commercial fibre-optic links. Nature, 2005, 438(7066): 343–346
4. Cheng C H, Chen Y C, Lin F Y. Chaos time delay signature suppression and bandwidth enhancement by electrical heterodyning. Optics Express, 2015, 23(3): 2308–2319
5. Torre M S, Masoller C, Shore K A. Numerical study of optical injection dynamics of vertical-cavity surface-emitting lasers. IEEE Journal of Quantum Electronics, 2004, 40(1): 25–30
6. Liao Y H, Liu J M, Lin F Y. Dynamical characteristics of a dual-beam optically injected semiconductor laser. IEEE Journal of Selected Topics in Quantum Electronics, 2013, 19(4): 1500606
7. Wieczorek S, Chow W W. Bifurcations and chaos in a semiconductor laser with coherent or noisy optical injection. Optics Communications, 2009, 282(12): 2367–2379
8. Tang S, Liu J M. Chaotic pulsing and quasi-periodic route to chaos in a semiconductor laser with delayed opto-electronic feedback. IEEE Journal of Quantum Electronics, 2001, 37(3): 329–336
9. Shibasaki N, Uchida A, Yoshimori S, Davis P. Characteristics of chaos synchronization in semiconductor lasers subject to polarization-rotated optical feedback. IEEE Journal of Quantum Electronics, 2006, 42(3): 342–350
10. Deng T, Xia G Q, Cao L P, Chen J G, Lin X D, Wu Z M. Bidirectional chaos synchronization and communication in semiconductor lasers with optoelectronic feedback. Optics Communications, 2009, 282(11): 2243–2249
11. Aoyama H, Tomida S, Shogenji R, Ohtsubo J. Chaos dynamics in vertical-cavity surface-emitting semiconductor lasers with polarization-selected optical feedback. Optics Communications, 2011, 284 (5): 1405–1411
12. Nguimdo R M, Verschaffelt G, Danckaert J, Van der Sande G. Fast photonic information processing using semiconductor lasers with delayed optical feedback: role of phase dynamics. Optics Express, 2014, 22(7): 8672–8686
13. Annovazzi-Lodi V, Aromataris G, Benedetti M. Multi-user private transmission with chaotic lasers. IEEE Journal of Quantum Electronics, 2012, 48(8): 1095–1101
14. Jiang N, Pan W, Yan L, Luo B, Zhang W, Xiang S, YangL, Zheng D. Chaos synchronization and communication in mutually coupled semiconductor lasers driven by a third laser. Journal of Lightwave Technology, 2010, 28(13): 1978–1986
15. Mirasso C R, Mulet J, Masoller C. Chaos shift-keying encryption in chaotic external-cavity semiconductor lasers using a single-receiver scheme. IEEE Photonics Technology Letters, 2002, 14(4): 456–458
16. Uchida A, Amano K, Inoue M, Hirano K, Naito S, Someya H, Oowada I, Kurashige T, Shiki M, Yoshimori S, Yoshimura K, Davis P. Fast physical random bit generation with chaotic semiconductor lasers. Nature Photonics, 2008, 2(12): 728–732
17. Butler T, Durkan C, Goulding D, Slepneva S, Kelleher B, Hegarty S P, Huyet G. Optical ultrafast random number generation at 1 Tb/s using a turbulent semiconductor ring cavity laser. Optics Letters, 2016, 41(2): 388–391
18. Lin F Y, Liu J M. Chaotic radar using nonlinear laser dynamics. IEEE Journal of Quantum Electronics, 2004, 40(6): 815–820
19. Wu W T, Liao Y H, Lin F Y. Noise suppressions in synchronized chaos lidars. Optics Express, 2010, 18(25): 26155–26162
20. Soriano M C, Colet P, Mirasso C R. Security implications of open- and closed-loop receivers in all-optical chaos-based communications. IEEE Photonics Technology Letters, 2009, 21(7): 426–428
21. Ursini L, Santagiustina M, Annovazzi-Lodi V. Enhancing chaotic communication performances by manchester coding. IEEE Photonics Technology Letters, 2008, 20(6): 401–403
22. Reidler I, Aviad Y, Rosenbluh M, Kanter I. Ultrahigh-speed random number generation based on a chaotic semiconductor laser. Physical Review Letters, 2009, 103(2): 024102–024105
23. Udaltsov V S, Goedgebuer J P, Larger L, Cuenot J B, Levy P, Rhodes W T. Cracking chaos-based encryption systems ruled by nonlinear time delay differential Equations. Physics Letters, 2003, 308(1): 54–60
24. Udaltsov, V S, Larger, L, Goedgebuer, J P, Locquet, A, Citrin, D S. Time delay identification in chaotic cryptosystems ruled by delay-differential equations. Journal of Optical Technology, 2005, 72(5): 373–377
25. Prokhorov M D, Ponomarenko V I, Karavaev A S, Bezruchko B P. Reconstruction of time-delayed feedback systems from time series. Physica D, Nonlinear Phenomena, 2005, 203(3–4): 209–223
26. Ortín, S, Gutiérrez, J M, Pesquera, L, Vasquez, H. Nonlinear dynamics extraction for time-delay systems using modular neural networks synchronization and prediction. Physica A Statistical Mechanics & Its Applications, 2005, 351(1): 133–141
27. Li S S, LiuQ, Chan S C. Distributed feedbacks for time-delay signature suppression of chaos generated from a semiconductor laser. IEEE Photonics Journal, 2012, 4(5): 1930–1935
28. Xiao P, Wu Z M, Wu J G, Jiang L, Deng T, Tang X, Fan L, Xia G Q. Time-delay signature concealment of chaotic output in a vertical-cavity surface-emitting laser with double variable-polarization optical feedback. Optics Communications, 2013, 286: 339–343
29. Lin H, Hong Y, Shore K A. Experimental study of time-delay signatures in vertical-cavity surface-emitting lasers subject to double-cavity polarization-rotated optical feedback. Journal of Lightwave Technology, 2014, 32(9): 1829–1836
30. Wu J G, Wu Z M, Tang X, Lin X D, Deng T, Xia G Q, Feng G Y. Simultaneous generation of two sets of time delay signature eliminated chaotic signals by using mutually coupled semiconductor lasers. IEEE Photonics Technology Letters, 2011, 23(12): 759–761
31. Li N, Pan W, Xiang S, Yan L, Luo B, Zou X. Loss of time delay signature in broadband cascade-coupled semiconductor lasers. IEEE Photonics Technology Letters, 2012, 24(23): 2187–2190
32. Liu H, Li N, Zhao Q. Photonic generation of polarization-resolved

wideband chaos with time-delay concealment in three-cascaded vertical-cavity surface-emitting lasers. Applied Optics, 2015, 54 (14): 4380–4387
33. Wu J G, Xia G Q, Tang X, Lin X D, Deng T, Fan L, Wu Z M. Time delay signature concealment of optical feedback induced chaos in an external cavity semiconductor laser. Optics Express, 2010, 18(7): 6661–6666
34. Wang A, Yang Y, Wang B, Zhang B, Li L, Wang Y. Generation of wideband chaos with suppressed time-delay signature by delayed self-interference. Optics Express, 2013, 21(7): 8701–8710
35. Wang A, Wang Y, Yang Y, Zhang M, Xu H, Wang B. Generation of flat-spectrum wideband chaos by fiber ring resonator. Applied Physics Letters, 2013, 102(3): 031112
36. Wang A, Wang B, Li L, Wang Y, Shore K A. Optical heterodyne generation of high-dimensional and broadband white chaos. IEEE Journal of Selected Topics in Quantum Electronics, 2015, 21: 1–10
37. Wu J G, Wu Z M, Xia G Q, Feng G Y. Evolution of time delay signature of chaos generated in a mutually delay-coupled semiconductor lasers system. Optics Express, 2012, 20(2): 1741–1753
38. Cheng M, Gao X, Deng L, Liu L, Deng Y, Fu S, Zhang M, Liu D. Time-delay concealment in a three-dimensional electro-optic chaos system. IEEE Photonics Technology Letters, 2015, 27(9): 1030–1033
39. Nguimdo R M, Colet P, Larger L, Pesquera L. Digital key for chaos communication performing time delay concealment. Physical Review Letters, 2011, 107(3): 034103
40. Gao X, Cheng M, Deng L, Liu L, Hu H, Liu D. A novel chaotic system with suppressed time-delay signature based on multiple electro-optic nonlinear loops. Nonlinear Dynamics, 2015, 82(1–2): 611–617
41. D'Huys O, Fischer I, Danckaert J, Vicente R. Spectral and correlation properties of rings of delay-coupled elements: comparing linear and nonlinear systems. Physical Review E: Statistical, Nonlinear, and Soft Matter Physics, 2012, 85(5): 056209

Xinhua Zhu received the B.S. and M.S. degrees in School of Optical and Electronic Information from the Huazhong University of Science and Technology, Wuhan, China, in 2014 and 2017, respectively. Now, he is an assistant engineer in Huawei. His research interests includes chaotic systems and secure communications.

Mengfan Cheng received the B.S. degree in information engineering, and the M.S. and Ph.D. degrees in computer science from the Huazhong University of Science and Technology, Wuhan, China, in 2005, 2007 and 2012, respectively. He was working as a Postdoctoral Researcher from 2013 to 2015. Now, he is a Lecturer in the School of Optical and Electronic Information, Huazhong University of Science and Technology. His research interests include fiber-optic communications, physical layer security, chaotic encryption, and chaotic synchronization.

Lei Deng received the B.S., M.S., and Ph. D. degrees in optoelectronics and information engineering from the Huazhong University of Science and Technology, Wuhan, China, in 2006, 2008 and 2012, respectively. He was in the Technical University of Denmark working toward the Ph.D. degree from 2010 to 2012. Now, he is an associate professor in the School of Optical and Electronic Information, Huazhong University of Science and Technology. His research interests include fiber-optic communications, advanced modulation formats and OFDM in radio-over-fiber (RoF) systems and next generation passive optical network (PON) systems.

Xingxing Jiang received the B.S. degree in optoelectronics and information engineering from the Huazhong University of Science and Technology, Wuhan, China, in 2015, where he is currently working toward the Ph.D. degree in optoelectronics and information engineering. His research interests include optical chaos system and fiber-optic communications.

Deming Liu received the Graduate degree from the Chengdu Institute of Telecommunication (now University of Electronic Science and Technology of China), Chengdu, China, in 1984. He is currently a Professor at the Huazhong University of Science and Technology, Wuhan, China. His research interests include optical access network, optical communication devices, and fiber-optic sensors.